

Supporting Information to:

Electrooxidation of C_4 polyols on platinum single-crystals: A computational and electrochemical study

Gabriela Soffiati^a, José L. Bott-Neto^{a,b}, Victor Y. Yukuhiro^{a,b}, Cléo T.G.V.M.T. Pires^a, Carlos C. Lima^a, Cinthia R. Zanata^c, Yuvraj Y. Birdja^d, Marc T. M. Koper^d, Miguel A. San-Miguel^a, Pablo S. Fernández^{a,b*}.

^a Chemistry Institute, State University of Campinas, PO Box 6154, 13083-970, Campinas SP, Brazil.

^b Center for Innovation on New Energies, University of Campinas, CEP 13083-841 Campinas, SP, Brazil.

^c Institute of Chemistry, Federal University of Mato Grosso do Sul, CEP 79070-900, Campo Grande, MS, Brazil

^d Leiden Institute of Chemistry, Leiden University, PO Box 9502, 2300, RA, Leiden, the Netherlands.

Corresponding Author

* email: pablosf@unicamp.br (P.S.F)

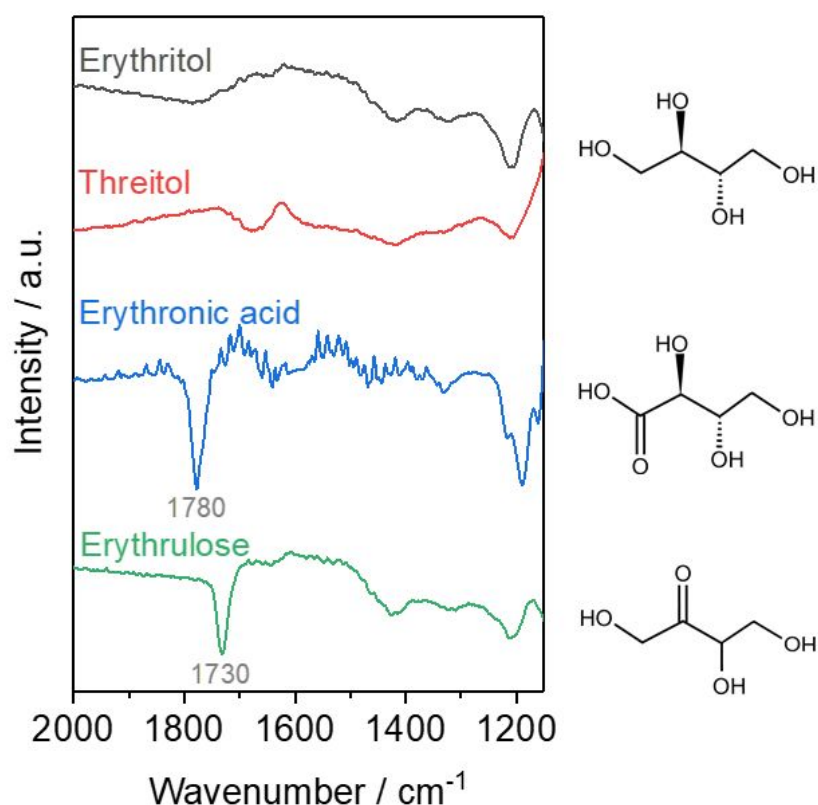


Figure S1: FTIR transmission spectra of erythritol, threitol, erythronic acid, erythrulose obtained in 0.1 mol.L⁻¹ HClO₄.

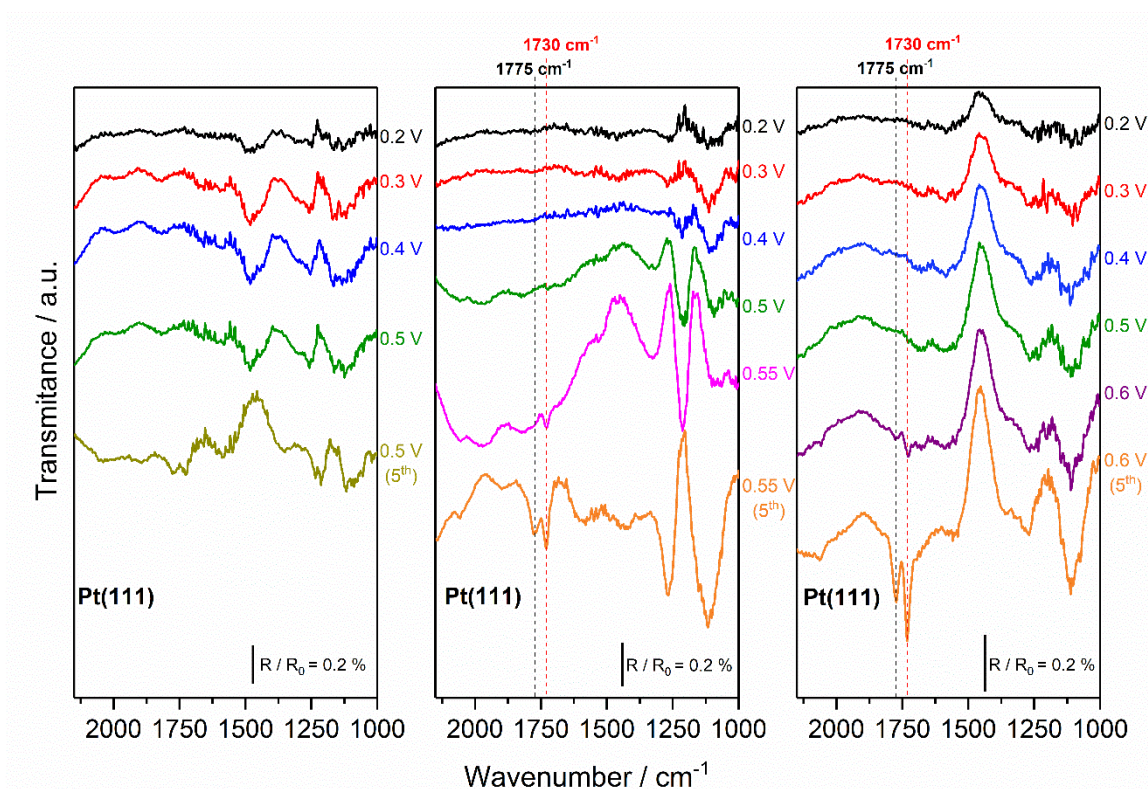


Figure S2. FTIR spectra taken at different electrochemical potentials (vs. RHE) for the electrooxidation of erythritol in $0.1 \text{ mol.L}^{-1} \text{ HClO}_4 + 0.005 \text{ mol.L}^{-1}$ on Pt(111).

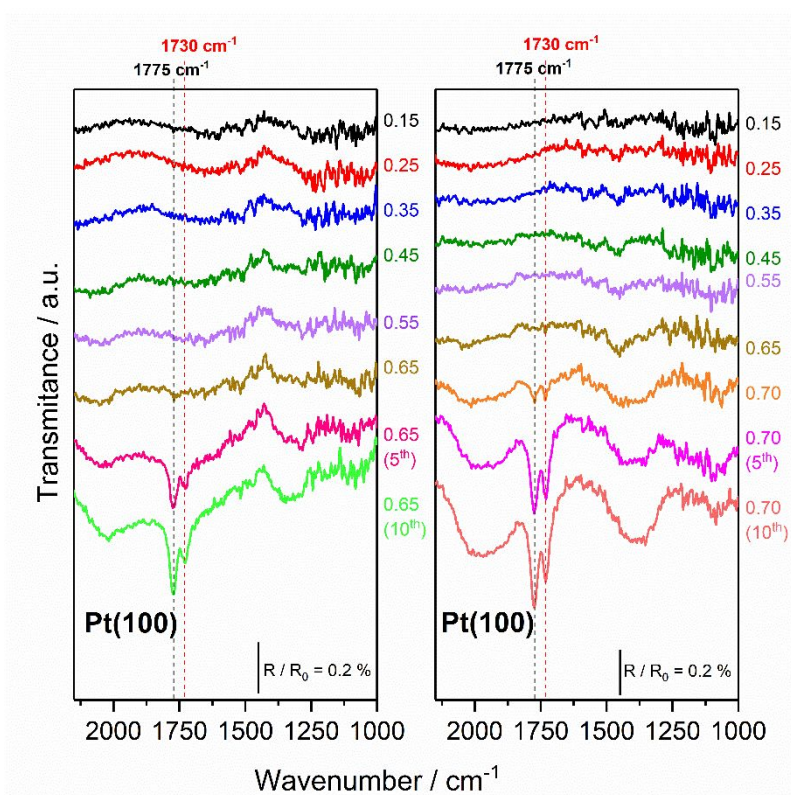


Figure S3. FTIR spectra taken at different electrochemical potentials (vs. RHE) for the electrooxidation of erythritol in $0.1 \text{ mol.L}^{-1} \text{ HClO}_4 + 0.005 \text{ mol.L}^{-1}$ on Pt(100).

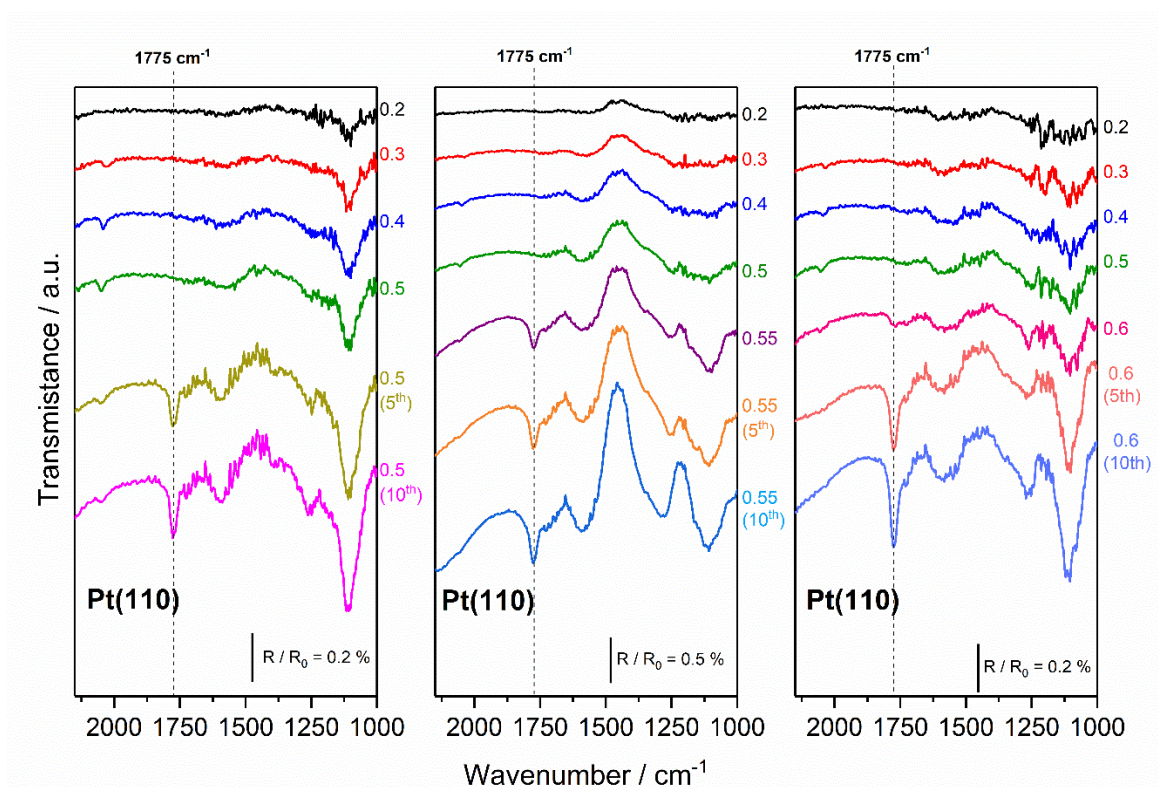


Figure S4. FTIR spectra taken at different electrochemical potentials (vs. RHE) for the electrooxidation of erythritol in 0.1 mol.L⁻¹ HClO₄ + 0.005 mol.L⁻¹ on Pt(110).

Electro-oxidation of erythritol and threitol: *in situ* FTIR

Figures S5 and S6 show the *in situ* FTIR spectra obtained during the electrooxidation of erythritol and threitol in 0.1 mol.L⁻¹ HClO₄ on the Pt(111), Pt(100) and Pt(110) surfaces. All spectra show bands at 2050 and 1810 cm⁻¹, which are related to the linearly (CO_L) and bridge-bonded (CO_B) carbon monoxide, respectively. Here, it is important to note that before recording the spectra, the electrode was cycled once in the presence of the polyol and then kept polarized at 0.1 V (vs. RHE) to stabilize the system (especially the thin layer), followed by taking the reference spectrum at 0.1 V. Consequently, the presence of the negative bands observed at typical wavenumber values of CO are related to the consumption of this species, which were produced in the previous potential cycling.

All three surfaces investigated show bands at 2342 and 1775 cm⁻¹ attributed to the formation of CO₂ and to the corresponding acids, respectively. For the Pt(111) electrode, between 0.1 and 0.6 V, an increase in the intensity of the bands of CO_L and CO_B species is observed. At 0.7 V, these bands

disappear completely, indicating that the formation of CO_2 is related to the oxidation of both species, among others.

On the other hand, for Pt (100) electrodes, it is observed that with the potential increase from 0.1 to 0.6 V, the intensity of the CO_B species decreases, while the intensity of the CO_L species increases, suggesting that the CO_B is converted to CO_L . For potentials above 0.7 V, the CO_L band is no longer observed, while the CO_B band remains constant with the potential, indicating that both species have been converted to CO_2 .

For Pt(110) there is also a decrease in the intensity of the positive bands for CO_L and CO_B with the potential increase up to 0.6 V. However, in contrast to the Pt(100) electrode, at higher potentials the main species is the CO_L .

It is worth to mention that the measurements in figures S5 and S6 were performed as described in the experimental part but using a Bruker Vertex 80 V IR spectrometer and a CaF_2 prism.

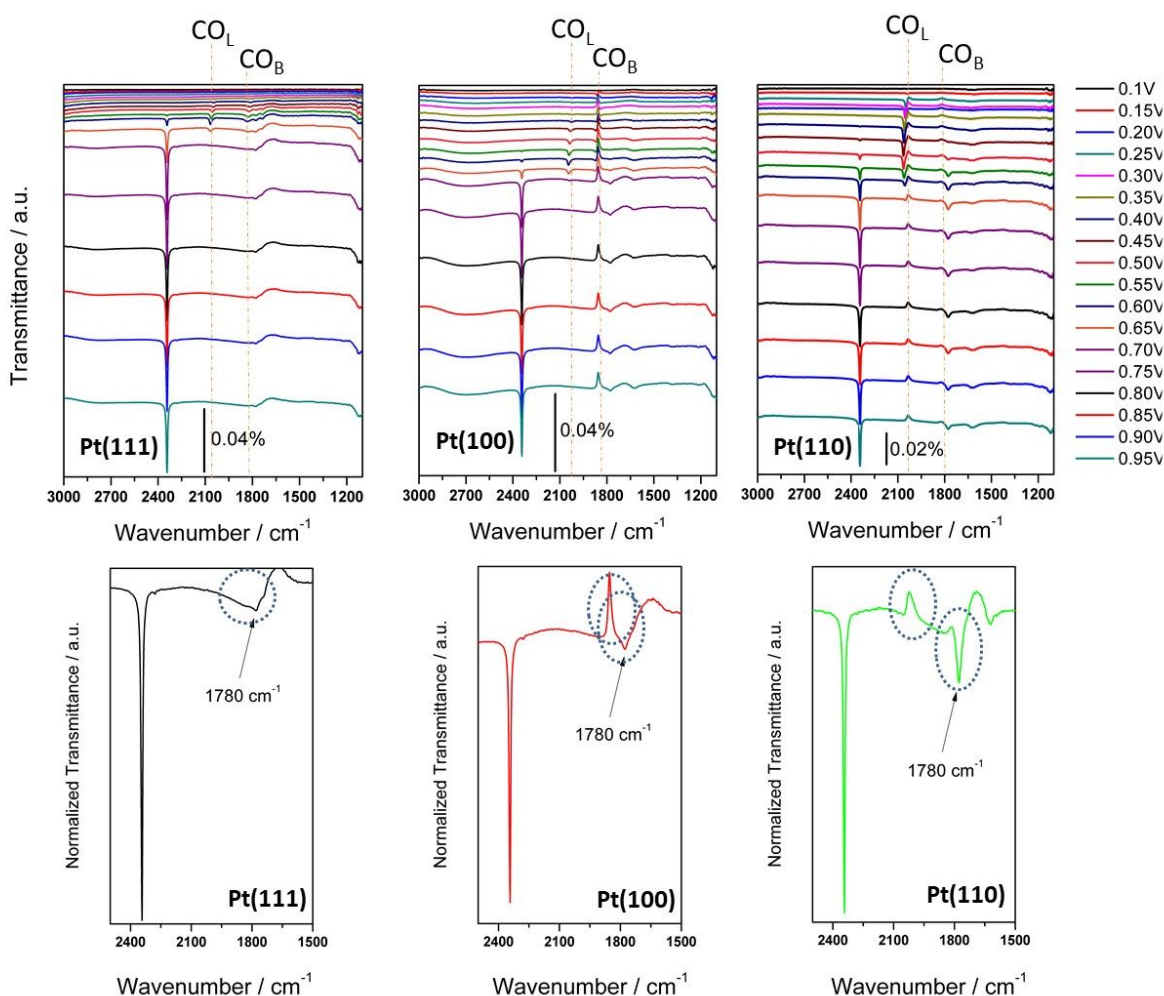


Figure S5: *In situ* FTIR spectra recorded for the electrooxidation of 5 mmol.L⁻¹ erythritol in 0.1 HClO₄ solution on Pt(111), Pt(100) and Pt(110). Enlarged view of spectra obtained at 0.7V (Below).

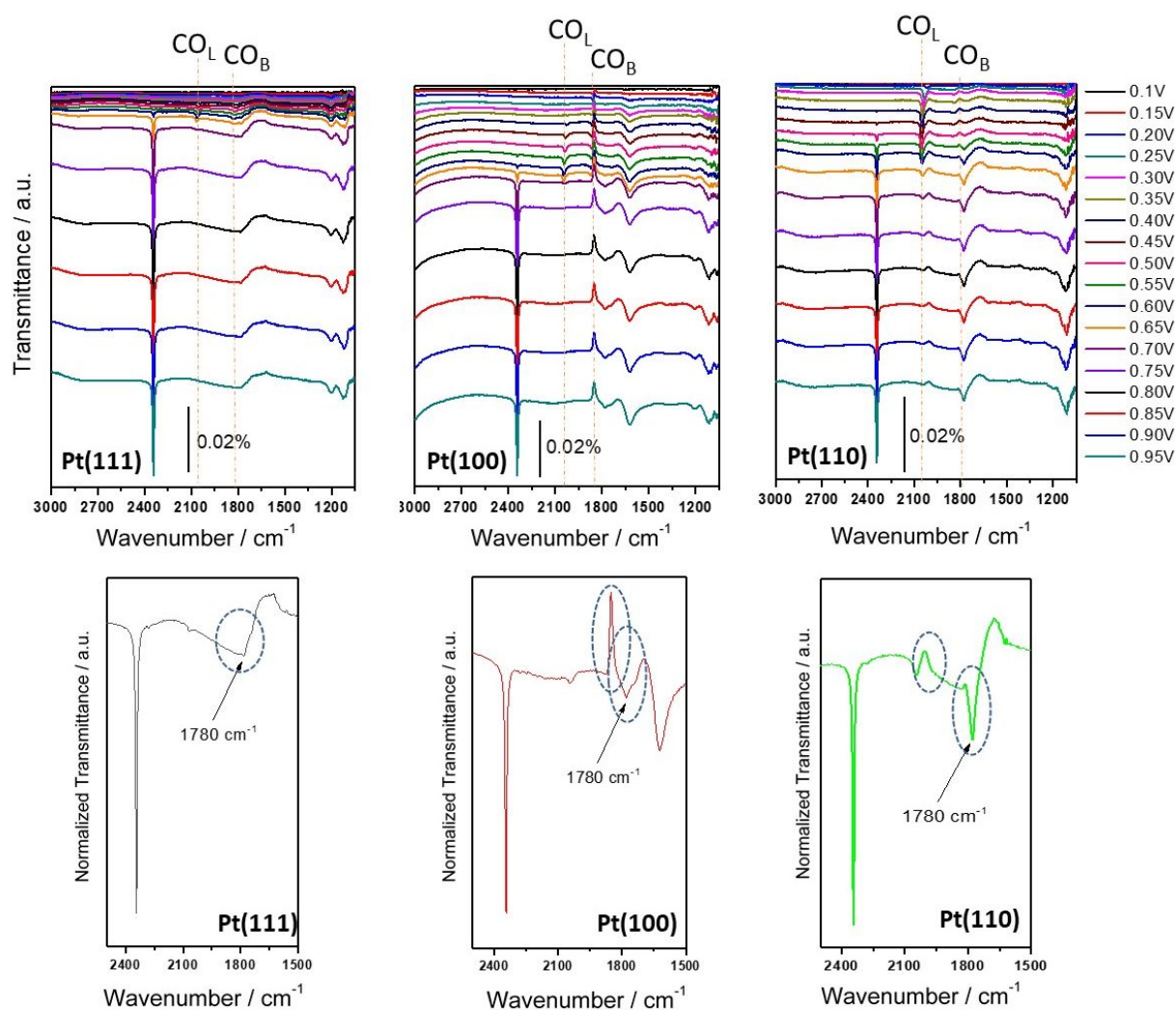


Figure S6: *In situ* FTIR spectra recorded for the electrooxidation of 5 mmol.L⁻¹ threitol in 0.1 HClO₄ solution on Pt(111), Pt(100) and Pt(110). Enlarged view of spectra obtained at 0.7V (Below).

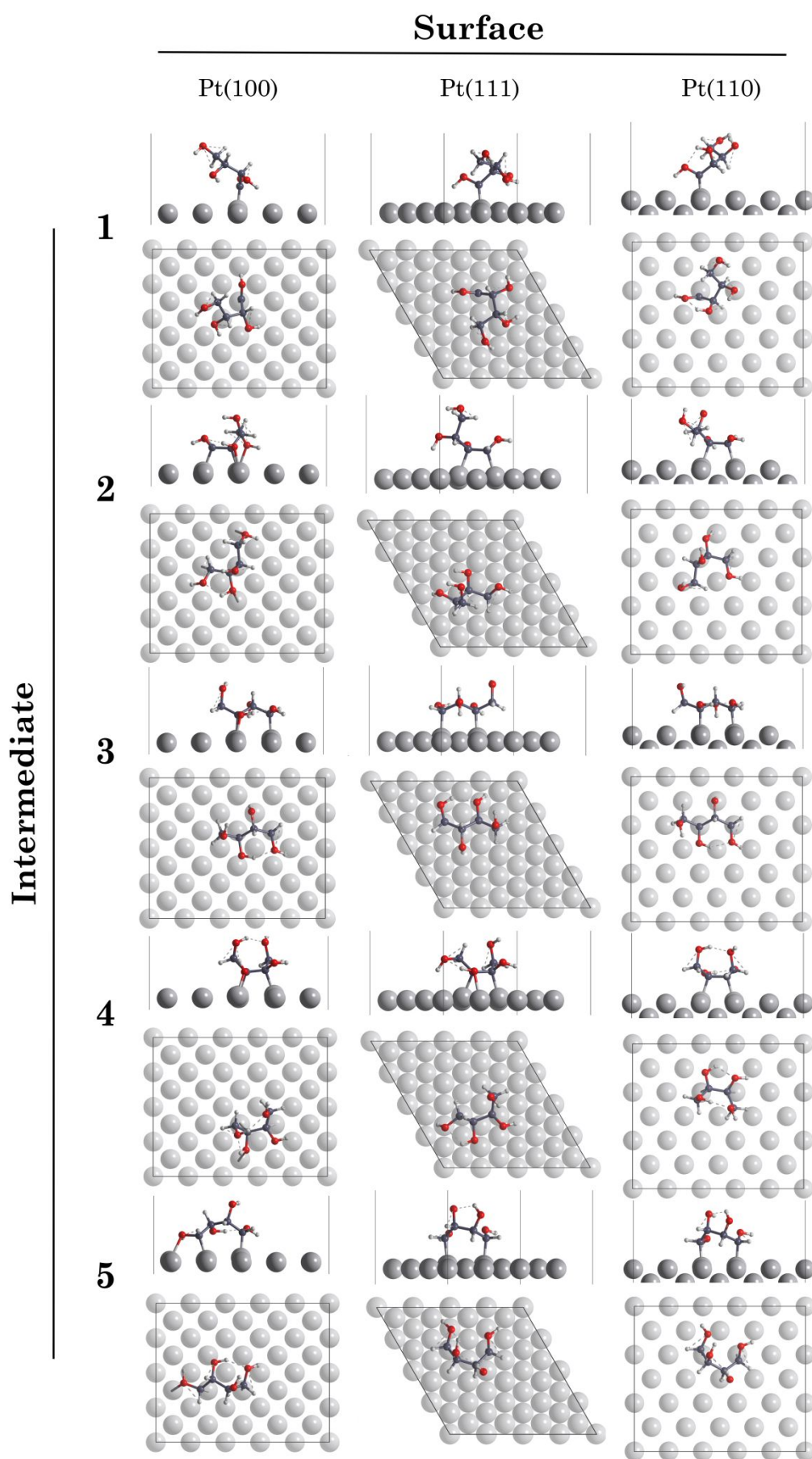


Figure S7. Top and side view of the less stable intermediate configurations for platinum (100), (111) and (110) surfaces calculated using the PBE approximation.

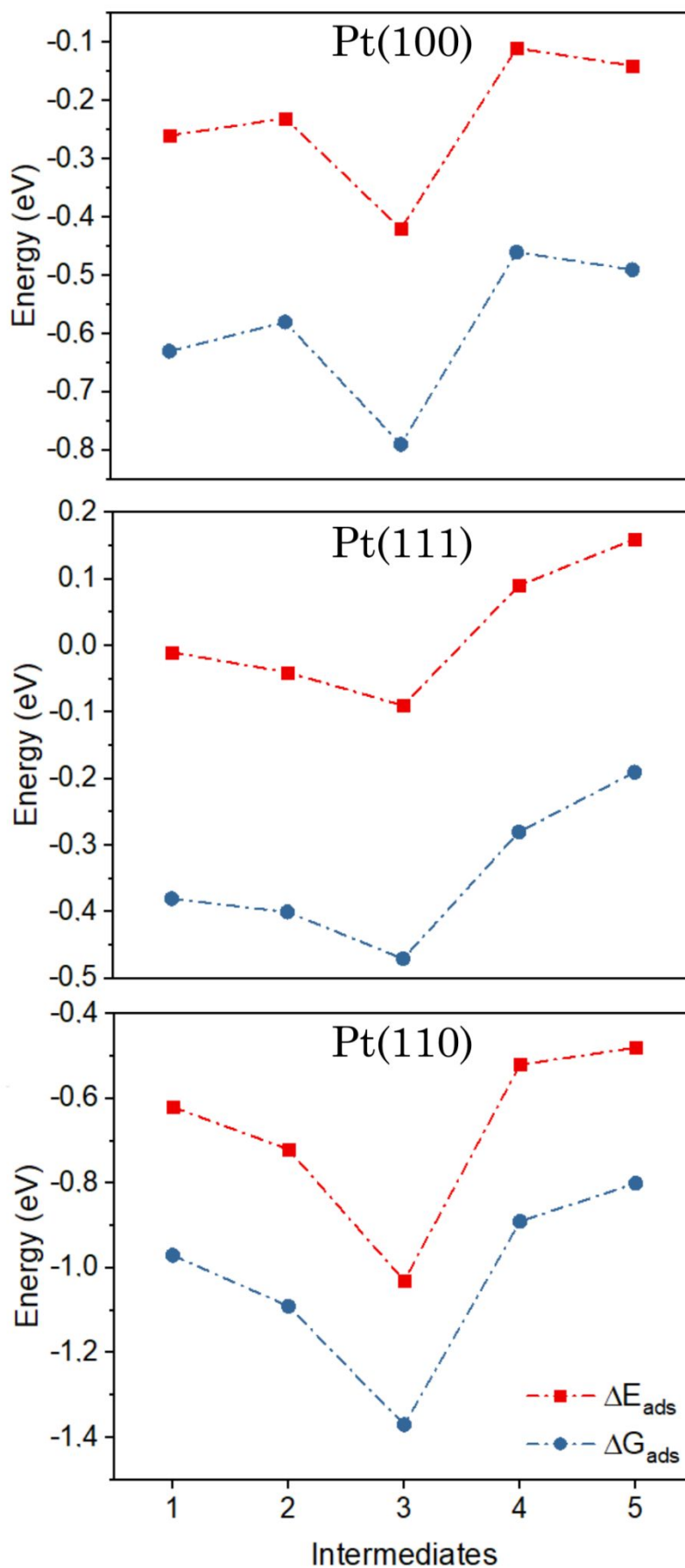


Figure S8. Comparison between the adsorption energies (ΔE_{ads}) and free adsorption energies (ΔG_{ads}) for intermediates using the PBE. The contribution of the vibrational zero-point energy

(ΔE_{ZPE}) and vibrational entropy corrections (ΔS) to the adsorption energies is similar, then the trends are the same for each structure independently of looking at the ΔE_{ads} or ΔG_{ads} data.